INTEGRATED PHOTONICS TECHNOLOGY FOR EARTH SCIENCE REMOTE-SENSING LIDAR

Fengqiao Sang[1], Joseph Fridlander[1], Victoria Rosborough[1], Simone Tommaso Šuran Brunelli[1], Jeffrey Chen[2], Kenji Numata[2], Randy Kawa[2], Mark Stephen[2], Larry Coldren[1], Jonathan Klamkin[1]

[1]Electrical and Computer Engineering Department, University of California, Santa Barbara, CA, USA
[2]NASA Goddard Space Flight Center, Greenbelt MD, USA

IGARSS 2021 - 2021 IEEE International Geoscience and Remote Sensing Symposium | 978-1-6654-0369-6/21/$31.00 ©2021 IEEE | DOI: 10.1109/IGARSS47720.2021.9553656

ABSTRACT

We present recent progress on a photonic integrated lidar system for carbon dioxide (CO_2) active remote sensing at 1572.335 nm. With integration, the cost, size, weight and power (CSWaP) of the system are significantly improved. System and subsystem level results are demonstrated.

Index Terms— Photonic integrated circuits, remote-sensing, lidar sensing

1. INTRODUCTION

Photonic integrated circuits (PICs) have been developed during the past few decades. With the growth of the data center and communication industries, integrated photonic technology has developed and matured rapidly in recent years. This gives us the opportunity to leverage PIC technology for remote science systems.

NASA Goddard Space Flight Center (GSFC) has spent several years developing a CO_2 remote sensing system based on laser absorption spectroscopy and the University of California, Santa Barbara (UCSB) is a leader in PIC technology [1-4]. We are collaborating to develop a PIC based CO_2 active lidar sensor based on NASA's current bench-top system [5,6]. The new system is designed and fabricated using an indium phosphide (InP) platform. One of the fabricated PICs, shown in Figure 1, has dimensions of 8300 µm by 700 µm. Integration significantly improved the cost, size, weight and power (CSWaP) of the lidar, which makes it ideal for implementation on small platforms, including CubeSats, drones, and space balloons.

In this work, we present the latest progress on this platform, including successful demonstration of laser wavelength stabilization and locking to the CO_2 line of interest, and the optical phase lock between the master and slave lasers, and the sampling of the CO_2 absorption line.

2. PIC PLATFORMS

There are many semiconductor material platforms useful for developing PIC technology. A popular one is silicon photonics (SiPh), which is currently growing quickly in both industry and academia. The SiPh platform uses silicon as its optical medium. It has the advantage of using complementary metal oxide semiconductor (CMOS) technology. CMOS reduces fabrication process development cost significantly and achieves sub-micron (down to tens of nanometers) resolution, also enabling monolithic integration of PICs and electronics integrated circuits. This makes it an ideal platform for data communication, where high speed electric and photonic communication interfaces are required. But the SiPh platform has a major disadvantage – silicon has an indirect bandgap and so is hard to be used to fabricate light sources, such as lasers [7]. Many researchers are trying to overcome this challenge via growth or bonding of direct bandgap materials on silicon, and though much progress has been made, but light sources of quality comparable to direct bandgap, group III-V materials, such as InP and GaAs, InGaAs and GaN, have not yet been achieved [8,9].

Another popular PIC platform is InP because it has the advantage that it can be used to make high-quality lasers, and high-speed modulators and photodiodes. The InP

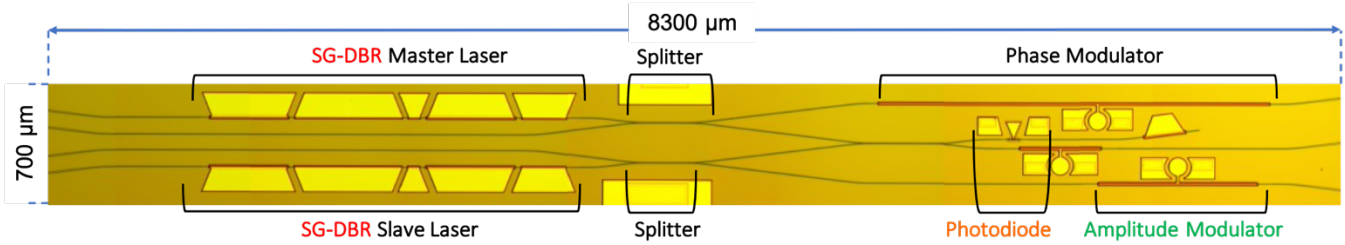

Figure 1: Microscope image of fabricated PIC.

platform has matured over the past decades and is widely used today for manufacturing lasers and modulators in the near infrared (NIR) region. Therefore, the groundwork has been laid to monolithically integrate all the necessary components together into a PIC. Compared to the SiPh platform, there are not that many InP multi-project wafer (MPW) services available for researchers and commercial use. Most InP foundries are only accessible for a company's internal use. Therefore, many researchers and companies choose to use academic nanofabrication facilities, such as the nanofabrication facility at UCSB. Those facilities do not provide a process design kit (PDK) for components, but do provide standard recipes for general-use tools. Under such circumstances, users get another degree of freedom when designing and optimizing their devices, but they also take the risk of not having a proven process with predictable performance.

3. ARCHITECTURE AND PIC DESIGN

The PIC was designed and fabricated based on an InP platform, using the two-laser architecture as shown in Figure 2. The first laser, the master laser, is locked to an external CO_2 reference cell, and the second laser, the slave laser, is locked to the master laser through an optical phase lock loop (OPLL).

The blue region in Figure 2 represents the monolithically integrated components, which include two lasers, a semiconductor optical amplifier (SOA), a

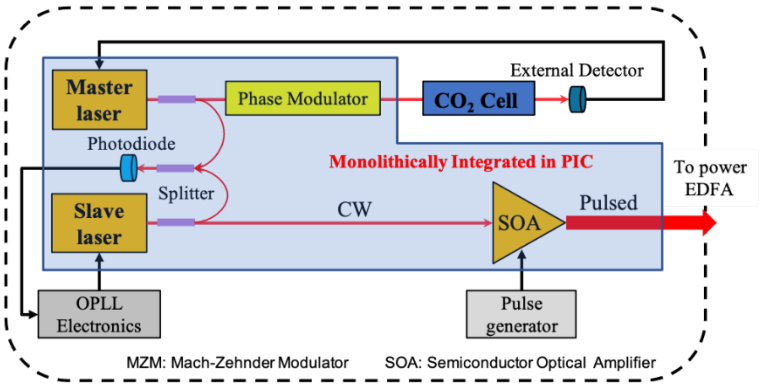

Figure 2: System architecture.

photodiode (PD), a phase modulator (PM), and passive splitters. Figure 1 shows one of the PICs that was designed and fabricated and later used for system level testing. On this PIC, both the master and slave lasers are sampled-grating distributed Bragg reflector (SG-DBR) lasers, which provide over 40 dB side mode suppression ratio (SMSR), and a 38 nm wavelength tuning range from 1566 nm to 1604 nm. Power splitting in the PIC was achieved with directional couplers instead of multi-mode interferometers (MMIs) to minimize reflections back into the laser. The phase modulator modulates the master laser output with a 125 MHz phase signal. The modulated master laser output passes through the CO_2 cell and an error signal is detected using coherent phase detection. The detected error signal is fed back to the master laser to stabilize the master laser to the CO_2 absorption line. The integrated photodiode detects the beat note signal between the master and slave lasers. The beat note signal goes to the OPLL electronics that are used to offset lock the slave laser to the master laser. The slave laser is stepped in frequency to map the CO_2 absorption line in the gas being sampled. The SOA after the slave laser is used as an amplitude modulator to generate a pulsed signal by modulating the SOA from zero bias where it acts as an optical absorber to forward bias where it acts as an optical amplifier.

4. TEST AND RESULT

We mounted the PIC shown in Figure 1 on a carrier for

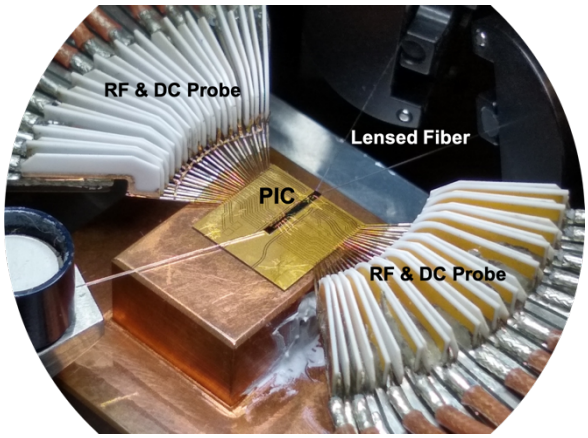

Figure 3: Camera image of PIC test setup.

system level testing, as shown in Figure 3. In the setup, two lensed fibers were used to externally couple the output light. An additional lensed fiber couples light from the back of the laser to monitor the output. The PIC was mounted in the center of the carrier and the device contacts were wire-bonded to the corresponding carrier pads to reroute the signal to RF & DC probes.

In this setup, we successfully stabilized the master laser to the CO_2 absorption peak at 1572.335 nm by modulating the on-chip phase modulator at 125 MHz with a modulation depth of π and feeding the error signal back into to the phase section of the laser. The comparison is shown in Figure 4(a). Without the feedback enabled, the peak-to-peak and standard deviation of the frequency drift over 10 minutes was 151 MHz and 30.2 MHz respectively. With the feedback enabled the peak-to-peak and standard deviation of the frequency drift over 10 minutes was reduced to 7.6 MHz and 1.54 MHz, an improvement of over 20 times.

In addition, the slave laser was successfully locked to the master laser. In Figure 4(b-c), the slave laser was locked to the master laser with offsets from 1 GHz to 15 GHz, and stabilization data was recorded and compared at a 2 GHz frequency offset. The results showed that with OPLL disabled and enabled, the peak-to-peak and standard deviation of the frequency drift improved from 1.99 GHz and 478 MHz to 30.26 MHz and 5.07 MHz respectively with 1 second gate times for 10 minutes measurement.

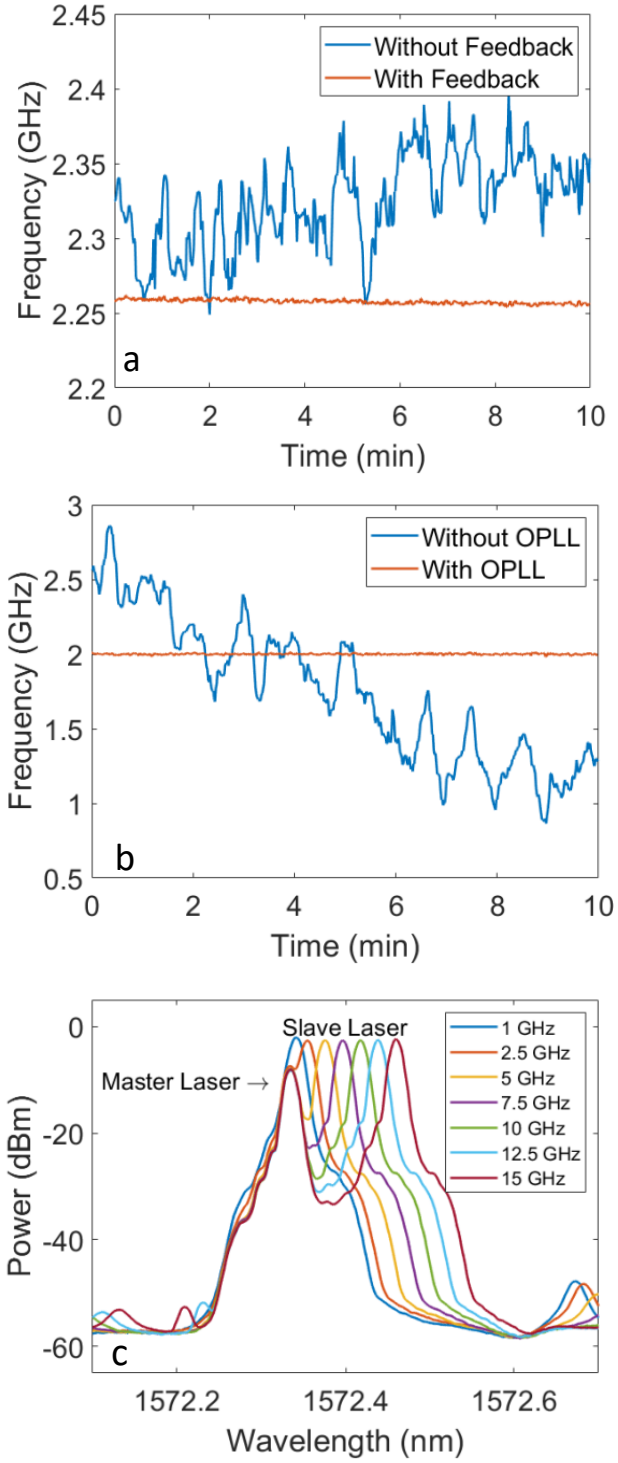

Figure 4: (a) Master laser wavelength stabilization. (b) Slave laser to master laser phase lock with 2 GHz offset. (c) Laser spectra with slave laser offset locked to master laser at 1 -15 GHz.

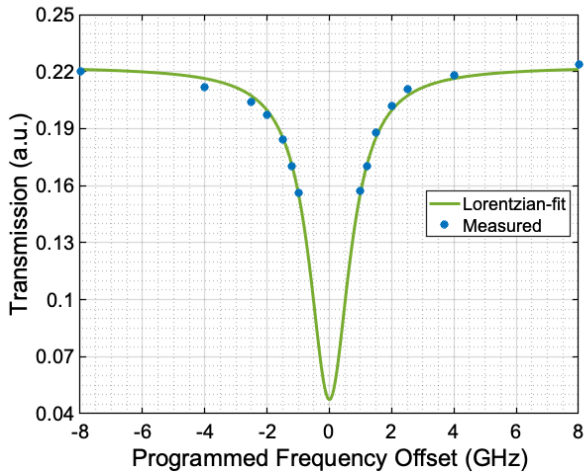

Figure 5: Measured absorption of the CO_2 test cell.

Finally, we demonstrated the sampling of the CO_2 absorption line around 1572.335 nm using a CO_2 test cell with a different pressure than the CO_2 reference cell. As illustrated in Figure 5, 14 wavelengths around 1572.335 nm were sampled. Each point is an average of 1000 measurements taken over 100 µs. The CO_2 absorption line was recoverable based on a Lorentzian fit of the sampled data points.

4. CONCLUSION

We designed and fabricated InP based PICs for a CO_2 remote active sensing application. We demonstrated efficient device operation and subsystem performance of the PIC, and also successfully demonstrated sampling of the CO_2 absorption line at 1572.335 nm. This work showed and proved the possibility of implementing PIC technology for remote active sensing applications, especially for small platforms, such as CubeSats and drones.

5. REFERENCES

[1] Klamkin, J., Zhao, H., Song, B., Liu, Y., Isaac, B., Pinna, S., ... & Coldren, L. (2018, October). Indium phosphide photonic integrated circuits: Technology and applications. In 2018 IEEE BiCMOS and Compound Semiconductor Integrated Circuits and Technology Symposium (BCICTS) (pp. 8-13). IEEE.

[2] Zhao, H., Pinna, S., Sang, F., Song, B., Brunelli, S. T. Š., Coldren, L. A., & Klamkin, J. (2019). High-power indium phosphide photonic integrated circuits. IEEE Journal of Selected Topics in Quantum Electronics, 25(6), 1-10.

[3] Stephen, M., Klamkin, J., Coldren, L., Fridlander, J., Rosborough, V., Sang, F., ... & Kawa, R. (2019, July). Integrated Micro-Photonics for Remote Earth Science Sensing (Impress) Lidar. In IGARSS 2019-2019 IEEE International Geoscience and Remote Sensing Symposium (pp. 4853-4856). IEEE.

[4] Fridlander, J., Rosborough, V., Sang, F., Nickerson, M., Chen, J., Numata, K., ... & Klamkin, J. (2020, May). Photonic Integrated Circuits for Precision Spectroscopy. In CLEO: Science and Innovations (pp. SF3O-3). Optical Society of America.

[5] Numata, K., Chen, J. R., & Wu, S. T. (2012). Precision and fast wavelength tuning of a dynamically phase-locked widely-tunable laser. Optics express, 20(13), 14234-14243.

[6] Numata, K., Chen, J. R., Wu, S. T., Abshire, J. B., & Krainak, M. A. (2011). Frequency stabilization of distributed-feedback laser diodes at 1572 nm for lidar measurements of atmospheric carbon dioxide. Applied optics, 50(7), 1047-1056.

[7] Canham, L. (2000). Gaining light from silicon. Nature, 408 (6811), 411-412.

[8] Liang, D., & Bowers, J. E. (2010). Recent progress in lasers on silicon. Nature photonics, 4(8), 511-517.

[9] Sysak, M. N., Liang, D., Jones, R., Kurczveil, G., Piels, M., Fiorentino, M., ... & Bowers, J. E. (2011). Hybrid silicon laser technology: A thermal perspective. IEEE Journal of Selected Topics in Quantum Electronics, 17(6), 1490-1498.

ACKNOWLEDGMENTS

The authors acknowledge funding from NASA's Earth Science Technology Office (ESTO) Advanced Component Technology (ACT) program. A portion of this work was performed in the UCSB Nanofabrication Facility.